UCID- 18156

Lawrence Livermore Laboratory

AN IMPROVED TANDEM MIRROR FUSION REACTOR

D. E. Baldwin, B. G. Logan and T. K. Fowler

April 1979

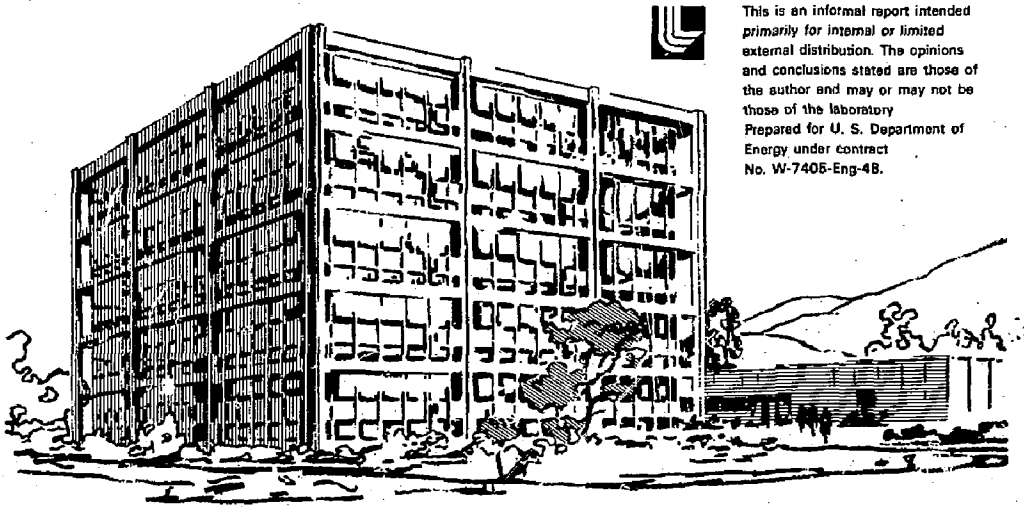

AN IMPROVED TANDEM MIRROR FUSION REACTOR

D. E. Baldwin, B. G. Logan and T. K. Fowler

Lawrence Livermore Laboratory, University of California

Livermore, California 94550

April 1979

ABSTRACT

An improved version of the tandem mirror fusion reactor is presented in which a power gain factor Q ~ 10 to 20 can be obtained at a new 100 MWe electrical output with much simpler technology in the end plugs. The improvement is obtained by raising the electron temperature in the end plugs well above that in the central cell (which would be ignited). The heating power required to maintain the high electron temperature is greatly reduced -- to 20 to 40 MW per plug -- by creating negative depressions in the potential that serve to thermally insulate electrons in the end plugs from those in the central cell. The overall concept and several proposed methods for creating the thermal barriers are discussed in Appendix A. A reactor example is discussed in Appendix B.

1. Introduction

This note describes an improved version of the tandem mirror fusion reactor concept that promises to yield a very high power gain (high Q) with much simpler technology in the end plugs. With the new scheme, it appears that in a full scale DT reactor producing 20 MW or more of fusion per meter of length, the total power consumed by the end plugs would be no more than 20 to 40 MW per plug, independent of the reactor length (the solenoidal plasma would be "ignited"). Then Q ~ 10 to 20 is readily possible at a few 100 MWe electrical output, with still higher Q values in larger systems.

The main point of the improved concept is to thermally insulate the end plug electrons from contact with those in the solenoid. Then, with ECRH or other auxiliary heating in the end plugs, the electron temperature can be much higher there than in the solenoid. With a high electron temperature in the plug, the usual tandem mirror potential barrier that plugs up ions leaking from the solenoid can be generated with a much lower plasma density n_p in the end plug. In fact, n_p can be less than n_c, the density in the solenoid, whereas in the original tandem mirror concept $n_p \gg n_c$.

It is this large reduction in the plug density that both reduces the power consumed in the plugs and opens up options for less demanding magnet and neutral beam technology in the end plugs. As the highest field on any conductor would be 12 T, the multifilamentary Nb_3Sn conductor already developed would suffice. Neutral beam energies could be around 200 Kev but

at greatly reduced power (and efficiency) requirements. While some ECRH heating is now required, it may be possible to use the 28 GC gyrotrons already in development, certainly in experiments and possibly in the reactor itself.

The concept is described in Appendix A. Briefly, the new feature is a depression in the plasma potential at the entrance to each end plug, as sketched in Fig. 1. This depression in the positive potential appears to the negatively charged electrons as a potential barrier and therefore serves as an electron "thermal barrier" between the end plugs and the solenoid. If we now heat the electrons in the plug at a rate faster than they can escape from the plug by collisions, the electron temperature would rise in the plug relative to that in the solenoid. Such electron temperature differences (along field lines) have been observed experimentally in the 2XIIB experiment,[1] with neutral beam heating only, and this fact has been explained by Monte Carlo computer simulations of the experiment.[2] Indeed, it was this observation that prompted the train of thought that eventually led to the new concept described here.

2. The Thermal Barrier

Several schemes for creating a thermal barrier have been considered. One such scheme is shown in Fig. 2. The first step is to add a simple mirror coil (circular) at the end of the solenoid; the thermal barrier region lies between this coil and the end plug. The simple mirror coil serves to throttle down the flow from the solenoid toward the plug.

In the absence of collisions, the density would then drop as the plasma expands in cross section as it emerges from the high magnetic field at the throat of the mirror coil. As is explained in the Appendix, this drop in density would create a potential depression, ϕ_b, for the same reason that the increase in density in the end plug creates an increase in potential there. It is this effect that we shall utilize to create ϕ_b, hence the thermal barrier.

However, to salvage the desired effect, it is necessary to add one other element to the system. As noted, the desired density drop occurs in the absence of collisions. The flowing plasma (which we may think of as "passing" particles) decreases in density as it passes through the field minimum and then rises again as it passes into the end plug. However, collisions among these passing particles -- ions and electrons -- cause some to be trapped between the magnetic mirrors. In time, because of the collisions, the trapped particle density would grow until the total pressure is equal to that in the solenoid.

To prevent this, we introduce a second coil producing a weak oscillating magnetic field in the neighborhood of the field minimum, B_b, in the barrier region between the simple mirror and the end plug. This oscillating field, at a frequency near the bounce frequency for trapped ions, serves to push the mirror fields back and forth axially, thereby jostling the trapped ions out of the magnetic well back into the solenoid and the end plug. This is a variant of the well known technique of "magnetic pumping". The required frequency is around 1 MHz -- readily

available commercially. The required power, mostly dissipative losses in the coil and cavity, is estimated to be at most a few megawatts, a small fraction of the total power input to the plugs.

The magnetic pumping scheme, as well as other approaches mentioned in Appendix A, are currently being analyzed to determine their effectiveness in preventing the accumulation of trapped ions in the thermal barrier. If results bear out expectations, it should ultimately be possible to reduce the ion density in the thermal barrier to about twice the passing ion density, of the order of (n_c/R_b), where $R_b = B_{mb}/B_b$ is the mirror ratio in the barrier. The electron density would drop accordingly; it is this that forces the potential to drop. Then, as is shown in Appendix A, Eq. (6),

$$\phi_b = T_{ec} \ln (R_b/\alpha) \tag{1}$$

where $\alpha \sim 1$ represents a collection of factors depending on details of the pumping process, and the end plug density becomes

$$n_p = n_c \exp\left(-\frac{\phi_b}{T_{ec}}\right) \exp \frac{\phi_b + \phi_c}{T_{ep}} \tag{2}$$

where n_p and n_c, and T_{ep} and T_{ec}, are the densities and electron temperatures in the end plug and solenoid, respectively. When $\phi_b = 0$,

Eq. (2) reduces to the usual tandem mirror relation between the density ratio n_p/n_c and the desired potential barrier ϕ_c to confine the ions in the solenoid. In that case, always $n_p > n_c$. But if ϕ_b is sufficiently large, and $T_{ep} >> T_{ec}$, one can obtain $n_p << n_c$; hence the advantage of the thermal barrier.

3. Reactor Design

Example reactor parameters are given in Appendix B. As one can see from Eqs. (1) and (2), the new parameters available to the reactor designer are the barrier mirror ratio R_b and the end plug electron temperature T_{ep}, which can be increased by ECRH heating. By increasing R_b and T_{ep}, n_p can be reduced more than an order of magnitude with the result that the midplane field in the end plug can be as small at 2 to 4 Tesla. This in turn permits a mirror ratio R_p in the end plug of 2 or more while restricting the field at the conductor to no more than 12 T. A large mirror ratio permits a smaller beam injection energy E_{inj} while satisfying the requirement that newly injected ions have energies above the ambipolar potential that could otherwise eject them promptly, namely,

$$E_{inj} > \frac{\phi_c + \phi_e}{R_p - 1} \quad . \tag{3}$$

Typically $\phi_c + \phi_e \approx 300$ Kev for DT ignition.

Another scheme for reducing E_{inj} still further is the "auxiliary cell", which is a second end plug with a density (and beam power) considerably below that of the main plug. This serves as a "voltage divider", whereby the potential drop across the main cell can be reduced by a factor of 2 or more, the remaining drop occurring across the auxiliary cell. Recent reactor studies at LLL[3] and the University of Wisconsin[4] have shown that an auxiliary cell can significantly reduce E_{inj} (and, correspondingly, the magnetic field) even without a thermal barrier. However, with a thermal barrier it does not appear that an auxiliary cell will be needed for a DT reactor.

4. Experimental Program

Fortunately, it appears that only modest modifications of the planned experiments are necessary to test the new thermal barrier concept. Moreover, by further reducing end losses that tend to mask other problems, introducing thermal barriers in these facilities should facilitate the study of radial transport in the solenoid and other physics issues not directly concerned with the end losses.

Introducing thermal barriers into TMX by the magnetic pumping method would require about 100 kW of 1 MHz ion pumping power (commercially available) together with 2 additional simple mirror coils. This should suffice to demonstrate a reduction of n_p to about the level of n_c (or rather, an increase of n_c to nearly equal n_p) and, with neutral beam heating only, a temperature difference $T_{ep} - T_{ec} \sim 0.5\ T_{ec}$. Such an

experiment would constitute a proof-of-principle. The later addition of about 1 MW of 28 GC ECRH heating, as is already planned, would further increase T_{ep} and increase $n\tau$ to about $10^{12} cm^{-3} sec$.

The addition of a thermal barrier to the proposed MFTF-B (tandem version of MFTF) would greatly improve its performance. Preliminary studies indicate that, with about 1 MW of 28 GC ECRH heating, one would be able to reach $n\tau \sim 10^{14} cm^{-3} sec$ at $T_{ci} \approx 10$ Kev. The 80 Kev MFTF beams would be used to heat the solenoid. In the end plugs, we would require 120 KV beam injection in the plugs, but one TFTR source for each plug may be sufficient. At 200 Kev injection, but again at low beam power, the performance would be still further improved.

We have also considered the implications of the thermal barrier concept for a DT-burning Mirror Next Step. Ideally, such a device would consist of 2 end plugs suitable for a full scale reactor together with a short length of ignited solenoid suitable for engineering development of the blanket. With the thermal barrier, we believe this ideal goal can be achieved and are now proceeding with conceptual studies of such a facility. If successful, this could lead to an Engineering Test Facility at moderate cost which could later be converted to a power-producing experimental reactor. Technology requirements are for the most part compatible with development programs in progress.

References

1. J. F. Clauser, Bull. Am. Phys. Soc, 23, 850 (1978).

2. T. D. Rognlien, Bull. Am. Phys. Soc., 23, 754 (1978).

3. G. A. Carlson and B. M. Boghosian, Parametric Studies of Tandem Mirror Reactors, Lawrence Livermore Laboratory, Rept. (in preparation).

4. R. W. Conn, private communication.

APPENDIX A

REDUCTION OF TANDEM MIRROR PLUG DENSITY BY FORMATION OF THERMAL BARRIERS

D. E. Baldwin and B. G. Logan

In tandem mirror (TM) confinement of fusion plasma, ions of a magnetized central cell are confined axially (or plugged) by the electrostatic potentials of more dense magnetic-mirror-confined plasmas.[1,2] When the electrons have an axially uniform temperature T_e, the creation of a potential difference ϕ_c requires a plug-to-central-cell density ratio given by

$$\frac{n_p}{n_c} = \exp\left(\frac{\phi_c}{T_e}\right) \tag{1}$$

(see Fig. 1). The degree to which the whole system floats above ground potential, fixing ϕ_e, is determined by the balance of total ion and electron loss.

Achievement of values of ϕ_c required for fusion is gained only logarithmically in the density ratio, whereas the ratio of central-cell fusion power density to that required to maintain the plugs varies as n_c^2/n_p^2. Elevation of the common T_e by auxiliary heating permits a decrease of n_p/n_c for fixed ϕ_c, but at the expense of raising the electron pressure above the ion pressure in the central cell, which then causes a decrease in the fusion power density for fixed total pressure.

These considerations have led to a conceptual TM reactor having severe technological requirements. To plug a central cell of density $\approx 10^{14}$ cm^{-3}, temperature ≈ 40 keV, and magnetic field ≈ 2 T requires high pressure plugs having peak fields ≈ 15 T and neutral-beam injection energies of order 600 keV with, or 1 to 2 MeV without, auxiliary electron heating.[3] In the following, we describe a means by which, for the same central cell conditions, the density and power requirements for the plugs might be dramatically reduced.

The essential idea is to raise the plug electron temperature above that in the central cell by auxiliary electron heating in the plugs. The heating power required is reduced by creating a locally negative potential dip between the plugs and central cell that thermally insulates the electrons of the two regions.

Consider the potential, magnetic field, and density profiles shown in Fig. 1. Electrons from the central cell pass through the plug and mix by weak collisions with those trapped in the higher potential. The resulting thermal contact is sufficient to allow only relatively small electron temperature differences between plug and central cell, even though considerable neutral-beam and auxiliary heating be applied to the plug.

The temperature difference is increased markedly by the addition of a (relatively negative) barrier potential $\phi_b \gtrsim T_{ec}$ (see Fig. 1) which would act as a thermal barrier between the plug and solenoid electrons. Power applied to the plug raises the temperature there (T_{ep}) relative to

that in the central cell (T_{ec}), which is close to the local ion temperature T_{ic}. Since plug electrons are confined by a potential $\phi_b + \phi_c$, the power/volume transferred between the plug and transiting central-cell electrons can be estimated[4]

$$P_{c\leftrightarrow p} \approx G_e \frac{n_p^2}{n\tau_{ee}} (T_{ep} - T_{ec}) \exp\left(-\frac{\phi_b + \phi_c}{T_{ep}}\right), \qquad (2)$$

where

$$n\tau_{ee} = \frac{m^{1/2}}{4\pi e^4 \ln\Lambda} (2T_{ep})^{3/2} = \frac{8.2 \times 10^9}{\ln\Lambda} T_{ep}^{3/2} \text{ keV} \cdot \text{cm}^{-3} \cdot \text{s},$$

and G_e of order unity is a weak function of potential and mirror ratio. (Accurate determination of this transfer rate is important for detailed reactor calculations and is being pursued by analytic and numerical means.) The power applied to the plug electrons eventually ends up in the central-cell electrons and contributes to their total power balance.

The barrier density n_b is related to n_c and n_p by

$$n_b = n_c \exp\left(-\frac{\phi_b}{T_{ec}}\right) = n_p \exp\left(-\frac{\phi_b + \phi_c}{T_{ep}}\right) \qquad (3a,b)$$

or, if we replace Eq. (1), there results

$$n_p = n_c \exp\left(-\frac{\phi_b}{T_{ec}} + \frac{\phi_b + \phi_c}{T_{ep}}\right). \qquad (4)$$

From Eq. (3a), generation of ϕ_b requires $n_b < n_c$. The ratio n_p/n_c can vary with parametric values, but it is always reduced below that given by

Eq. (1). This reduction results both from the explicit presence of ϕ_b in Eq. (4) and in the insulation permitting $T_{ep} > T_{ec}$. Most importantly, the power required to maintain the plug has dropped by n_p^2.

The depression in the central-cell density required in Eq. (3a) might be achieved by one of several means; three possible ones are described below. In each case, we take as an irreducible minimum ion density in the barrier that which is due to central-cell ions streaming through the locally negative potential. Assume this drop in potential is also accompanied by a drop in the magnetic field by a factor R_b. Then, by particle flux conservation, when $\phi_b > T_{ec}$, the density of central-cell ions passing through region b is given by

$$n_c(b) = \frac{n_c}{R_b}\left(\frac{T_{ic}}{\pi\phi_b}\right)^{1/2} . \tag{5}$$

Added to this will be the density of ions trapped in ϕ_b, and it will be most important that their accumulation be prevented. If the total barrier ion density n_b (passing plus trapped) is normalized to the density of passing ions, i.e., $n_b = g_b n_c(b)$, then from Eqs. (3a) and (5) we find

$$\left(\frac{T_{ic}}{\phi_b}\right)^{1/2} \exp\left(\frac{\phi_b}{T_{ec}}\right) = \frac{R_b\sqrt{\pi}}{g_b} . \tag{6}$$

This result points up the importance of a large mirror ratio in the barrier region and a nearly complete pumpout of the trapped thermal ions from this region (for which $g_b \to 1$). Two considerations are important in assessing

reasonable estimates for g_b: (i) The degree to which specific pumpout mechanisms can compete with collisional trapping, and (ii) The questions of microstability of the resulting distributions. Because of the number of these physics uncertainties, g_b must at this time be considered a variable physics parameter that must be of order unity to be useful.

As a first method for thermal ion pumpout, we propose a transit-time heating of locally trapped ions. For this purpose, a circular coil would be inserted into the central cell to generate a local mirror (see Figs. 1 and 2). The mirror ratio R_b in Eq. (5) is then the ratio B_{mb}/B_b. Parallel heating of locally trapped ions will result when there is applied a parallel force oscillating at the ion bounce frequency. Examples of such a force are a parallel electric field (difficult at high density) or small oscillation of the position, depth, or axial extent of the local magnetic well. The first method has been successfully used to pump some electrons out of the Phoenix mirror machine,[5] creating a rise in the ambipolar potential. The second method is most easily described in the case where $\underset{\sim}{B}(z,t) = \underset{\sim}{B}[z_0(t)]$, for then in the oscillating frame

$$\frac{\partial f}{\partial t} + v_{\parallel}(\varepsilon,\mu,z)\,\frac{\partial f}{\partial z} = \frac{q}{m}\,\ddot{z}_0\,\frac{\partial f}{\partial \varepsilon} \quad , \tag{7}$$

where (ε,μ) are the particle energy and magnetic moment, and the oscillation frequency is tuned to the bounce frequency of the bulk of trapped ions. The absorbed power density for this heating, which ends up as heating to the whole central cell, is that which competes with the trapping rate for passing central-cell ions into the potential well, a formula similar to Eq. (2),

$$P_{pump} \approx G_i \frac{n_b n_c(b)}{(n\tau)_{ii}} T_{ic} \ , \tag{8}$$

where $(n\tau)_{ii} = 5 \times 10^{11} \, T_{ic}^{3/2}/\ln\Lambda \ cm^3 \cdot s$, and $G_i \approx 1$.

Determination of the degree to which thermal ions can be pumped out by this means against collisional filling and the amplitude of the required fields depends upon details of the electrostatic and magnetic well shapes, resonance frequencies, their widths and overlap, the applied frequency spectrum, island formation in phase space, etc. Modeling of this process in both the diffusion, or Fokker-Planck, limit and by single particles with a Monte Carlo collision process are underway at Livermore.

The microstability question does not appear to pose a limit on the ion density in the barrier region. For $k_\perp = 0$ ion-ion and ion-acoustic modes, treating the passing ions as two beams of velocity $u_D = (2\phi_b/m_i)^{1/2}$ and the $v_\parallel$-integrated trapped ion distribution as nearly independent of parallel velocity, we find the local dispersion relation

$$D(\omega) = 1 + \frac{4\pi e^2 n_c(b)}{m_i k_\parallel^2} \left\{ g_b \frac{m_i}{m_e} \left(\frac{m_e}{T_{ec}} + \pi i \left. \frac{\partial f_e}{\partial v_\parallel} \right|_{\frac{\omega}{k_\parallel}} \right) + (g_b - 1) \frac{k_\parallel^2}{k_\parallel^2 u_b^2 - \omega^2} + \pi i \left. \frac{\partial f_b}{\partial v} \right|_{\frac{\omega}{k_\parallel}} \right)$$
$$- \frac{k_\parallel^2}{2} \left[\frac{1}{(\omega - k_\parallel u_b)^2} + \frac{1}{(\omega + k_\parallel u_b)^2} \right] \Bigg\} = 0 \ . \tag{9}$$

The low-ω ion-ion mode is stable when Re $D(\omega=0) > 0$, true even at $g_b = 1$ when $2\phi_b > T_c$. This correlation would still permit a negative energy wave destabilized by electron Landau damping (the ion-acoustic mode). A sufficient condition for stability is a combination of the density and

distribution of trapped ions satisfying Im D > 0, or

$$(g_b - 1)\frac{\partial f_b}{\partial v_\parallel} > - g_b \frac{m_i}{m_e}\frac{\partial f_e}{\partial v_\parallel} \quad , \tag{10}$$

which represents a low density, rising gently to match the passing particle distribution. For much the same reasons that these $k_\perp = 0$ modes are stable, Drummond and Rosenbluth[6] find that, for nearly equal ion and electron temperatures, $k_\perp \neq 0$ modes in a magnetic field require relative drifts of some 15 to 20 times the ion thermal spread. For purpose of reactor evaluation, we have assumed the value $g_b = 2$, for which all of these beam-driven modes are stabilized.

Potential MHD modes in the barrier region are the firehose, requiring for stability

$$\beta_{\parallel} - \beta_\perp \leq 2 \quad , \tag{11}$$

and the flute interchange, requiring for stability

$$\int \frac{ds}{B^2}(p_\perp + p_\parallel) K_\psi > 0 \quad , \tag{12}$$

where K_ψ is the component of the line curvature normal to the constant-pressure flux surface, and the integration runs the entire TM length. We rely on positive curvature plugs to stabilize the negative-curvature regions joining high-field plugs with the uniform central cell, as in the conventional TM.[7] Of possible concern is the added destabilization of the

barrier region. Using model fields and pressure profiles, we find the minimum-B plugs of mirror ratio 2, ellipticity 30, and $\beta_\perp \approx 0.4$ can line-average-stabilize a mirror ratio 10 barrier region of $\beta_\parallel \approx 1$. The curvature constraint is more stringent than the firehose, but is easily satisfied.

A second pumpout mechanism is related to the first in that it entails a local mirror region embedded at each end of the solenoid. In this scheme, the minimum of the barrier region in Fig. 1(b) would periodically be raised to the peak mirror value, so that all trapped thermal ions would escape. When returned to its minimum value, the barrier regions would remain empty of trapped ions for a fraction of a collision time, at which time the cycle would be repeated. The potential barrier offered by such a barrier region would not be constant in time, so that this method might require a pair of such barriers, operating out of phase.

As regards issues of stability, this means of emptying the barrier region would be expected to be similar to the preceding one.

Finally, in the stream-stabilized mode of 2XIIB operation, it frequently occurred that stream density outside the mirror on the upstream side exceeded the hot ion density between the mirrors.[8] At the same time, there appeared at the mirror throat a marked density dip, by a factor of 5 to 10. It was argued that the ion cyclotron rf precluded accumulation of ions at the magnetic maximum by a process similar to rf plugging. If this interpretation stands up, one would expect a similar profile between the plugs and central cell in the Tandem Mirror Experiment (TMX). Furthermore,

it might be possible to extend this technique for barrier generation to reactor conditions, either by internally or externally generated rf.

An addition that might be necessary in some situations is the confinement of anisotropic, hot electrons in the barrier region. When added to the right side of Eq. (3a), the presence of such electrons would give a larger ϕ_b for a given n_b, further reducing the power transfer between the plug and central-cell electrons. However, the power necessary to sustain these hot electrons, presumably generated by electron-cyclotron resonance heating, must compete with the electron-electron scattering rate. Provided good pumpout can be achieved, $g_b \approx 1$ to 2, we find nearly equal power is required not to generate anisotropic electrons, but to bulk heat the plug electrons as described above.

In summary, we have emphasized the utility of barrier potentials between the central cell and the plugs of a TM. Of crucial importance are the questions of how the barrier is formed and how completely the accumulation of thermal ions can be prevented. The most favorable conditions would permit a TM reactor with dramatically improved parameters. The degree to which this ideal can be approached will take time to evaluate, and probably we have not yet found the best scheme for efficiently pumping thermal ions. The potential improvements to be gained from this approach are so great as to warrant a thorough theoretical and experimental study.

References

1. G. I. Dimov, V. V. Zakaidakov, and M. E. Kishinevsky, Fiz. Plasmy 2, 597 (1976); Proc. 6th Inter. Conf. Plasma Physics and Cont. Nucl. Fusion Res., Berchtesgaden, (1976), Paper C4.

2. T. K. Fowler and B. G. Logan, Comments Plasma Phys. II, 167 (1977).

3. R. W. Moir, et al., Preliminary Design Study of the Tandem Mirror Reactor, Lawrence Livermore Laboratory, Rept. UCRL-52302 (1977).

4. V. P. Pastukhov, Nucl. Fusion 14, 3 (1974).

5. E. Thompson, et al., Proc. 10th Meeting Div. of Plasma Phys. APS, 3D-4 (1968).

6. W. E. Drummond and M. N. Rosenbluth, Phys. Fluids 5, 1507 (1962).

7. D. E. Baldwin, et al., Proc. 7th Inter. Conf. on Plasma Physics and Cont. Nucl. Fusion Res., Innsbruck (1978), CN-37-J-4.

8. F. H. Coensgen, et al., MX Major Project Proposal, Lawrence Livermore Laboratory, Rept. LLL-Prop-142 (1976).

Appendix B

TMR Examples Utilizing Thermal Barriers

B. G. Logan

In this first calculation of TMR parameters with thermal barriers, we pursue a primary goal of reducing plug technology requirements - neutral beam voltage, power, and plug magnetic fields. In addition we look for higher fusion power density in the center cell to raise the blanket power loading. To exploit the thermal barrier principle described in the previous appendix, we will necessarily introduce new reactor components - specifically, ECRH or other electron heating in the plugs, simple mirror coils, and an ion pump in the thermal barrier such as one of those described in Appendix A. While we believe the different technologies required by these new components are available today or in the near future, the aim of this section is to give a preliminary assessment of the new TMR parameters, rather than give a detailed design of these new reactor components which will come later. Since some of the reactor parameters will be influenced by the chosen type of electron heating and ion pumping, however, we assume ECRH for the electron heating and compressional ion pumping using pulsed coils to guide the reactor design in these first examples. The physics and engineering of compressional pumping is straightforward; at the same time, it is too soon to tell if R.F. pumping will ultimately prove better.

The axial profiles of potential, field and electron density are as shown in Fig. 2 of Appendix A, except the field is allowed to dip in the transition regions between the thermal barrier mirror cells and the minimum-B mirror cells. Thus there are four peaks in the magnetic field at each end of the center cell, with the outer two peaks formed by a minimum-B magnet and the inner two peaks generated by a pair of circular coils, all

superconducting. The ion pumping in the thermal barrier cells is achieved by periodically pulsing normal copper coils inside the blanket at the local field minima in the thermal barrier cells and in the transition regions. After a characteristic time

$$\tau_g \simeq \frac{2.5 \times 10^{10} T_{ic}^{3/2}(\text{keV})}{1/2\, n_b\ (\text{cm}^{-3})} \left(\frac{\frac{\phi_b}{T_{ic}} + 1}{2 R_b} \right)^{2/3} \simeq 0.1 - 0.5 \text{ sec.} \qquad (1)$$

for trapped ions to accumulate by collisions to a density equal to the passing ion density (barrier fill factor $g_b \to 2$) in the local potential well of the thermal barriers, the pulsed coils at the barrier cell midplanes are pulsed on, raising the barrier midplane field B_b temporarily to the barrier mirror field B_{mb}, thus allowing the trapped ions to escape. At the same time, lower field pulsed coils at the field minima in the transition regions are pulsed on to lower the field and ion density there, temporarily holding the same electron thermal barrier there while the main thermal barrier mirror cells are being purged. The pulsed coils in the transition regions need produce only ~0.6 T bucking field while the pulsed coils at the barrier cell midplanes must add ~3.4 T, so only the power dissipation in the pulsed barrier coils is important. The pulse duration τ_{ON} is short compared to $\tau_g (\tau_{ON} \simeq 30$ ms) so that ions don't trap in the barrier cell as the barrier midplane field is restored to its steady state value, and so that the duty factor for the pulsed coils is small. To reduce the stored magnetic energy in the pulsed barrier coils, the static mirror fields B_{mb} are kept small, usually less than the minimum-B mirror fields B_{mp}, but larger than the center cell field B_c. Higher temperature reactor regimes with longer τ_g are also desired to allow longer pulse times τ_{ON} for the pulsed coils.

For TMR reactor regimes of interest, the ECRH power required to maintain the plug electron temperature higher than the center cell electron temperature, given by eq. 2 in App. A, is the dominant power input to the plasma. Therefore to maximize Q, reactor designs should minimize this ECRH power. Neglecting the plug neutral beam power and the ion pump power for the moment, we can write

$$Q_{ECRH} \simeq \frac{P_{fusion}}{P_{cp}} \left(\frac{V_c}{2V_p}\right) \tag{2}$$

Using eq. 2 in App. A for the ECRH power P_{cp}, we obtain

$$Q_{ECRH} \simeq \frac{1}{4} (n\tau)_{ee} \left(\frac{n_c}{n_p}\right)^2 \exp\left(\frac{\phi_b + \phi_c}{T_{ep}}\right) \langle\sigma v\rangle_{DT} \left(\frac{E_F}{T_{ep} - T_{ec}}\right)\left(\frac{V_c}{2 V_p}\right) \tag{3}$$

where E_F = 17,600 keV is the energy release per fusion, and $(n\tau)_{ee} \simeq 4 \times 10^8 T_{ep}^{3/2}$ at $\ln \Lambda_{ee} \simeq 20$. Thus using eq. 4 in App. A for the density ratio n_p/n_c, we have

$$Q_{ECRH} \simeq 10^8 \, T_{ep}^{1/2} \, e^{\frac{2\phi_b}{T_{ec}}} \, e^{\frac{-(\phi_b + \phi_c)}{T_{ep}}} \langle\sigma v\rangle_{DT} \left(\frac{17{,}600}{1 - \frac{T_{ec}}{T_{ep}}}\right)\left(\frac{V_c}{2V_p}\right). \tag{4}$$

Then, using eq. 6 of App. A for the ratio of barrier potential to center cell electron temperature ϕ_b/T_{ec}, and taking $T_{ec} \simeq T_{ic}$, we get

$$Q_{ECRH} \simeq 10^8\, T_{ep}^{1/2} \left(\frac{R_b}{q_b}\sqrt{\frac{\pi\phi_b}{T_{ic}}}\right)^2 e^{\frac{-(\phi_b+\phi_c)}{T_{ep}}} \langle \sigma v\rangle_{DT} \left(\frac{17600}{\frac{T_{ec}}{1-\frac{T_{ec}}{T_{ep}}}}\right)\left(\frac{V_c}{2V_p}\right) \quad (5)$$

Eq. 5 shows that Q increases as T_{ep} increases, so we choose the maximum

$$T_{ep}(max) \simeq \phi_b + \phi_c \quad (keV) \quad (6)$$

for marginal validity of our model, which assumes the trapped plug electrons to be Maxwellian up to the local potential barrier $\phi_b + \phi_c$ which confines them. At high reactor temperatures where $\phi_b + \phi_c$ is large, one must check that the synchrotron radiation power in the plugs

$$P_{sync} \simeq 6 \times 10^{-20} B_p^2(T)(1 - \beta_p)\, T_{ep}^2\, n_p\, 2V_p\, K_L \ (watts) \quad (7)$$

is small compared to P_{cp}, as is true in all the examples we will consider. K_L is the radiation reabsorption parameter which is $<<$ 1 for $T_{ep}<200$ keV, but rapidly approaches unity above 200 keV.

Since the hot electrons extend to their local potential barrier peak $\phi_b + \phi_c$ located at the thermal barrier midplane, the ECRH power can be applied anywhere between the thermal barrier midplane and the ion plug midplane, where $f_{ce} = f_\mu$ and where $f_{pe} < f_{ce}$:

$$B_{res} = 3.6 \times 10^{-11} f_\mu \quad (tesla) \quad (8)$$

$$n_e < n_{cutoff} \leq 10^{13} B_{res}^2 \quad (9)$$

Typically, the latter condition eq. (9) restricts us to $f_\mu \simeq 60$ GHz, where $B_{res} \simeq 2T$ halfway up or down the barrier mirrors which are adjacent to the plugs. At the present time, however, the next step in ECRH gyrotron tube development beyond the present 28 GHz tubes is planned to be 110 GHz. This frequency allows cutoff densities above the plug densities in our examples, although we would still prefer to apply the ECRH to the transition regions near the outer barrier mirrors where $B_{res} \simeq 3.6$ T, to avoid crowding and interference with the plug neutral beams. We note that microwave absorption increases with T_e, so that at reactor temperatures the absorption can be nearly 100% even without microwave cavities[1], simplifying microwave antenna design and reducing stray microwave power.

As indicated in eq. (5), Q increases as the square of the mirror ratio $R_b = B_{mb}/B_b$ in the thermal barrier, so large mirror ratios there are desired. An upper limit on R_b is set by either MHD flute stability (eq. 12 in App. A) or by the firehose instability (eq. 11 in App. A), the former being more restrictive on R_b for our reactor examples. An analytic approximation to eq. 12 of App. A gives approximately

$$0.4\, R_b^{3/2} \lesssim \left\{ \begin{array}{l} 3.168 \text{ for } R_p = 2 \\ 0.916 \text{ for } R_p = 3 \end{array} \right\} R_c^2 \left(\frac{L_{mb}}{L_{mp}}\right)\left(\frac{\beta_p}{\beta_c}\right)\sqrt{\frac{\pi T_{ic}}{\phi_b}}\left(\frac{2}{g_b}\right) \qquad (10)$$

for minimum-B plug magnets with vacuum mirror ratio $R_p = B_{mp}/B_p$ and maximum ellipticity $= r_{max}/r_{min} = 30$, where

$$R_c = \frac{B_{mb}}{B_c} \qquad (11)$$

---

(1) Miklos Porkolab, UCRL-52634, Dec. 1978.

is the vacuum mirror ratio from the barrier mirror to the center cell, and L_{mb}/L_{mp} is the ratio of mirror-to-mirror lengths of the barrier and plug. For the large $R_b \simeq 7$-10 allowed by eq. 10 for $R_p = 2$, the dominant beta-weighted bad curvature contribution to eq. 12 in App. A comes from the barrier midplanes even when the center cell beta β_c is high, since $\beta_{\parallel} \simeq 1$ in the barrier at these mirror ratios. The limit on β_c is set instead by ballooning, for which Newcomb and Pearlstein[2] have calculated β_c limits up to 0.75 for an axisymmetric simple mirror appropriate to the region between the center cell and the inner barrier mirror. Note that for a fixed maximum ellipticity that can be accommodated in a minimum-B magnet geometry, the stabilizing force of the plugs is reduced at higher R_p. Thus lower R_p is desired to allow higher R_b and Q; however, lower R_p also raises the ambipolar cutoff potential $(\phi_e + \phi_c)/[(R_p/\sqrt{1 - \beta_p}) - 1]$ in the plugs, forcing higher neutral beam injection energies E_{inj}. We choose $R_p = 2$ (vacuum) for the minimum-B plug magnet in our examples, as a compromise. Note also in eq. 10 that R_b, and therefore Q, would also increase with increasing R_c, or increasing barrier mirror field B_{mb}. However, practical limits on the stored magnetic energy required in the pulsed barrier coils set $B_{mb} \leq 4T$ with compressional pumping. This consideration does not apply to R.F. pumping, which can use B_{mb} up to 10T, easily obtainable with circular coils. The higher barrier mirror ratios thus possible with R. F. pumping would nearly offset the higher $g_b \cong 2\ \phi_b/T_{ic} \simeq 5$ that results from diffusive R. F. parallel heating.

The plug beta β_p which appears in eq. 10 is limited by Drift-Cyclotron-Loss-Cone (DCLC) instabilities in that the number of ion

---

(2) W. A. Newcomb and L. D. Pearlstein, UCID-16736 (1975).

gyroradii in the plug radius (r_p/a_i) required for DCLC stability is a monotonically increasing function of plug beta for a given average ion energy $\bar{E}_p$ and T_{ep}. (See Fig. B1 for hydrogen and $E_p + T_{ep} = 1$ MeV, for example.) Higher β_p allows higher R_b (up to some limit of β_p of order unity at which eq. 10 derived in the low beta limit would no longer apply) and also enhances the effective plug mirror ratio $R_p/\sqrt{1 - \beta_p}$, reducing the ambipolar cutoff potential and required neutral beam voltages. As hydrogen ions in the plugs allow higher β_p due to their smaller gyroradius, the plugs are assumed to be hydrogen. Hydrogen plugs also greatly reduce neutron fluxes in the plugs, easing magnet shielding and extending neutral beam life against neutron damage.

As the thermal barriers allow ECRH heating of the plug electron temperature T_{ep} sufficient to give any desired ϕ_c, we choose a sufficiently high ϕ_c (and therefore T_{ep} by eq. (6)) to give ignition in the center cell with respect to the center cell ion end losses:

$$\frac{1}{4} n_c^2 \langle\sigma v\rangle_{DT} E_\alpha f_{\alpha i} = \left(\frac{n_c^2}{(n\tau)_c}\right)(\phi_c + T_{ic}) + \frac{1}{2} n_c^2 \langle\sigma v\rangle_{DT} \bar{E}_r$$

$$+ \left(\frac{n_c^2}{(n\tau)_c} + \frac{1}{2} n_c^2 \langle\sigma v\rangle_{DT}\right)(3/2\ T_{ic}) \frac{f_{cx}}{f_{ion}}$$

$$+ \frac{n_c^2\ 3/2\ (T_{ic} - T_{ec})}{10^{12}\ T_{ec}^{3/2}} \qquad (12)$$

where $$\frac{\phi_c}{T_{ic}} = \ln\left[\frac{(n\tau)_c}{5 \times 10^{10}\ T_{ic}^{3/2}\left(\frac{\phi_c}{T_{ic}}\right)}\right],$$

E_α = 3520 keV is the alpha energy, $f_{\alpha i}$ is the fraction of alpha energy transferred to the ions (see fig. B2 of Fokker-Planck calculations of $f_{\alpha i}$ by Marvin Rensink),

$$E_r \simeq 45 + 3/2\ T_{ic} \tag{13}$$

is approximately the mean reacting ion energy, and where $f_{cx}/f_{ion} \simeq 0.6$ is the ratio of charge-exchange to ionization for low energy neutrals impinging on the center cell plasma which is thick compared to the neutral mean-free-path. As the ECRH power to the trapped plug electrons is transferred to the center cell electrons, T_{ec} would generally exceed T_{ic}, raising the center cell electron potential ϕ_e together with the plug ambipolar cutoff potential, and also increasing the center cell plasma pressure for a given fusion power density. Since ϕ_c is no longer tied to T_{ec}, we can improve the fusion power density for a given field and lower plug potentials by cooling the center cell electrons to offset the transferred ECRH power and any excess alpha heating of electrons, to keep $T_{ec} \leq T_{ic}$. There are many ways to do this, but perhaps the simplest way is to release a cold electron current I_s from a grid-controlled cathode on the end wall, removing $I_s T_{ec}$ power from the center cell electron population. The cold electron current which would result in $T_{ec} \simeq T_{ic}$ can be calculated from the electron energy balance:

$$\frac{n_c^2}{(n\tau)_c}(\phi_e + T_{ec})\ V_c + I_s(T_{ec}) + \frac{1}{2}\, n_c^2 \langle\sigma v\rangle_{DT}(\phi_e + T_{ec})\ V_c$$

$$= \frac{1}{4}\, n_c^2 \langle\sigma v\rangle_{DT} E_\alpha\, f_{\alpha e}\, V_c + \frac{P_{fusion}\ (MW)\ 10^3/q}{Q} \tag{14}$$

$$+ \frac{n_c^2\ 3/2\ (T_{ic} - T_{ec})}{10^{12}\ T_{ec}^{3/2}} V_c \qquad (15)$$

where we set the last term on the RHS to zero. Eq. (15) can then be solved to give

$$\frac{I_s}{I_c} = (n\tau)_c \langle \sigma v \rangle_{DT} \left[\frac{200}{T_{ec}} + \frac{E_{\alpha o} f_{\alpha e}}{4\ T_{ec}} - \frac{1}{2} \left(1 + \frac{\phi_e}{T_{ec}}\right) \right] - \left(1 + \frac{\phi_e}{T_{ec}}\right) \qquad (16)$$

where f_{α_e} is the fraction of alpha energy transferred to electrons (Fig. B2),

$$I_c = \frac{q\ n_c^2\ V_c}{(n\tau)_c} \qquad (17)$$

is the center cell ion loss current, and where the electron potential is given by

$$\frac{\phi_e}{T_{ec}} = \ln \left[\frac{(n\tau)_c / (1 + I_s/I_c)}{5 \times 10^8 T_{ec}^{3/2} \left(\frac{\phi_e}{T_{ec}}\right)} \right] . \qquad (18)$$

Note that ϕ_e/T_{ec} is also reduced by the cold electron current I_s, a beneficial effect. While we find a cold electron current I_s is not essential to achieving a satisfactory reactor performance, the improvements obtainable with such a current, particularly the reduction in the plug

ambipolar cutoff potential, and therefore minimum neutral beam injection energy, may be worth the trouble. To some extent the same effects may occur anyway with a finite secondary electron emission from the direct converter.

The ignition condition, which is given by eq. (12), essentially determines $(n\tau)_c$ as a function of T_{ic}. As $T_{ec} = T_{ic}$ (up until $I_s \to 0$ at high T_{ec} by eq. 16, at which point T_{ec} drops below T_{ic}), the potentials ϕ_e, ϕ_b and ϕ_c are all increasing, not quite linearily, with T_{ic}. By eq. 6, T_{ep} is also increasing with T_{ic}. Minimum neutral beam voltages are constrained to be above the ambipolar cutoff energy, so beam voltage, is also scaling up with T_{ic}. Thus T_{ic} is the primary variable controlling the TMR parameters, and so we will work out parameters for three cases: (1) T_{ic} = 20 keV, (2) T_{ic} = 40 keV, and (3) T_{ic} = 60 keV. One consideration is that $(n\tau)_c$ for ignition by eq. 12 is minimum ($\simeq 9 \times 10^{14} cm^{-3} sec$) at $T_{ic} \simeq 40$ keV, assuming end losses dominate over radial losses, as we have done. If instead radial losses were dominant, the minimum $(n\tau)_c$ for ignition would occur around 25 keV, since radial loss energy per particle would be 3/2 T instead of ϕ + T per particle lost out the ends. Since the addition of circular mirrors for the thermal barrier will virtually eliminate neoclassical radial loss, and since finite beta may stabilize drift waves, the prospects for small radial loss in this type of tandem are very good.

What remains to complete the reactor design is to determine the volume ratio $V_c/2V_p$, which appears in the expression for Q. This volume ratio is determined by three constraints:

(1) Total fusion power:

$$P_{fusion} = 2\pi r_w \Gamma L_c \quad (MW), \tag{19}$$

where r_w is the first wall radius in meters, Γ the first wall neutron wall loading in MW/m^2, and L_c is the center cell length in meters. Specifying a combination of r_w and Γ is also equivalent to specifying the fusion power per unit length P_{fusion}/L_c.

(2) Conservation of magnetic flux:

$$r_c = r_p \left(\frac{n_p}{n_c}\right)^{1/4} \left(\frac{0.8\,\bar{E}_p + T_{ep}}{T_{ic} + T_{ec} + \bar{T}_\alpha}\right)^{1/4} \left(\frac{1 - \beta_p}{1 - \beta_c}\right)^{1/4} \left(\frac{\beta_c}{\beta_p}\right)^{1/4} \tag{20}$$

where $$\bar{T}_\alpha \simeq 8.3 \times 10^{10} \langle\sigma v\rangle_{DT} \bar{E}_\alpha f_{\alpha e} T_{ec}^{3/2} \text{ (keV)} \tag{21}$$

is the average perpendicular hot alpha energy per unit center cell density.

(3) Maximum conductor field in the plug magnet:

$$B_{max} = \frac{B_{mp}}{\eta_m} = B_c \left(\frac{R_p}{\eta_m}\right)\left(\frac{n_p}{n_c}\right)^{1/2} \left(\frac{0.8\,\bar{E}_p + T_{ep}}{T_{ic} + T_{ec} + \bar{T}_\alpha}\right)^{1/2} \left(\frac{\beta_c}{\beta_p}\right)^{1/2} \tag{22}$$

where $\eta_m = B_{max}/B_{mp} = 0.75$ is the magnet mirror efficiency, and where the center cell field is given by

$$B_c = \sqrt{\frac{n_c(T_{ic} + T_{ec} + \bar{T}_\alpha)}{2.5 \times 10^{15} \beta_c}}\ , \tag{23}$$

Where the center cell density is related to the center cell radius r_c

through the wall loading constraint (1) as

$$n_c = r_c^{-1}(m)\sqrt{\frac{3.55 \times 10^{12} r_w \Gamma}{\langle\sigma v\rangle_{DT}}} \quad cm^{-3} \tag{24}$$

where $\langle\sigma v\rangle_{DT}$ is the fusion reaction rate in $cm^3 sec^{-1}$. Solving eq. (22) for r_c using eq. (23) with (24), we get

$$r_c = \frac{7.54 \times 10^{-10}}{B_{max}^2}\left(\frac{0.8\,\bar{E}_p + T_{ep}}{\beta_p}\right)\left(\frac{r_w \Gamma}{\langle\sigma v\rangle_{DT}}\right)^{1/2}\left(\frac{n_p}{n_c}\right)\left(\frac{R_p}{n_m}\right)(m). \tag{25}$$

Although the plug ions extend out to the mirrors where L_{mp} is long compared to the plug plasma radius r_p in general, the axial density profile when finite beta is taken into account gives an equivalent plug volume which can be approximated as a sphere of radius r_p, in computing power losses such as P_{cp} which scale as n_p^2:

$$V_p \simeq (4\pi/3)\, r_p^3. \tag{26}$$

Thus the volume ratio becomes

$$\frac{V_c}{2V_p} = \frac{\pi r_c^{\,2} L_c}{2(4\pi/3) r_p^{\,3}} = \frac{3}{8}\left(\frac{r_c}{r_p}\right)^3 \frac{L_c}{r_c}\ , \tag{27}$$

which, using eq. (25) and eq. (20), becomes

$$\frac{V_c}{2V_p} = 6.4 \times 10^7 \left(\frac{\eta_m B_{max}}{R_p}\right)^2 \frac{P_{fusion}^{(MW)}}{(r_w r)^{3/2}} \left(\frac{n_c}{n_p}\right)^{1/4} \frac{\langle\sigma v\rangle_{DT}^{1/2}}{(T_{ic} + T_{ec} + \bar{T}_\alpha)^{3/4}} \cdot$$

$$\frac{\beta_p^{1/4} \beta_c^{3/4}}{(0.8\bar{E}_p + T_{ep})^{1/4}} \left(\frac{1 - \beta_p}{1 - \beta_c}\right)^{3/4} \qquad (28)$$

Substituting this expression into eq. (5) for Q_{ECRH}, taking $R_p = 2$, and using

$$\frac{n_c}{n_b} = \left(\frac{R_b}{g_b}\sqrt{\frac{\pi\phi_b}{T_{ic}}}\right) \frac{10.2}{g_b} \left(\frac{B_{mb}}{\eta_m B_{max}}\right)^{0.8} \left(\frac{L_{mb}}{L_{mp}}\right)^{0.4} \left(\frac{0.8\,\bar{E}_p + T_{ep}}{T_{ic} + T_{ec} + \bar{T}_\alpha}\right)^{0.4} e^{.4\left(\frac{\phi_b + \phi_c}{T_{ep}}\right)} \qquad (29)$$

obtained from the MHD constraint, eq. 10, and eqs. (23), (24) and (25), we obtain finally

$$Q_{ECRH} = 5.2 \times 10^{21} \frac{T_{ep}^{0.5}}{g_b^{2.25}} B_{mb}^{1.8} (\eta_m B_{max})^{0.2} \left(\frac{L_{mb}}{L_{mp}}\right)^{0.9} \frac{e^{-0.35\frac{\phi_b + \phi_c}{T_{ep}}}}{\left(1 - \frac{T_{ec}}{T_{ep}}\right)}$$

$$\cdot \frac{\langle\sigma v\rangle_{DT}^{1.5}}{(T_{ic} + T_{ec} + \bar{T}_\alpha)^{1.65}} (0.8\,\bar{E}_p + T_{ep})^{0.65} \frac{P_{fusion}}{(r_w r)^{3/2}} \beta_p^{1/4} \beta_c^{3/4}$$

$$\left(\frac{1 - \beta_p}{1 - \beta_c}\right)^{3/4} \cdot \qquad (30)$$

We can now evaluate Q_{ECRH} and other plasma parameters for the three cases T_{ic} = 20 keV, 40 keV and 50 keV, holding fixed the following:

(1) $P_{fusion} = 1500$ MW

(2) $r_w \Gamma = 4$ MW/m $\rightarrow L_c = 48$ m, $P_{fusion}/L_c = 31$ MW/m.

(3) $B_{max} = 12$ T

(4) $\eta_m = 0.75$ ($B_{mp} = 9$ T)

(5) $R_p = 2$ ($B_p = 4.5$ T)

(6) Yin-Yang ellipticity = 30

(7) $L_{mb} = L_{mp}$

(8) $\beta_c = 0.75$ (ballooning limit)

(9) $E_{inj} \simeq 1.5\ (\phi_e + \phi_c)/\left[(R_p/\sqrt{1 - \beta_p}) - 1\right]$, rounding off to the lowest "canonical" voltage.

(10) $T_{ep} = \phi_b + \phi_c$

(11) $\bar{E}_p \simeq 2.5\ E_{inj}$ (small electron drag)

(12) $B_{mb} = 4$T

(13) $g_b = 2$

(14) $r_{wall} = r_c + 2\rho_\alpha$ (*in computing* Γ)

Instead of Q_{ECRH}, we are more interested in the overall reactor Q which includes the neutral beam power trapped in the plugs P_{NB} and the ion pump power P_{pump} absorbed by the plasma ions:

$$Q = \frac{P_{fusion}}{P_{ECRH} + P_{NB} + P_{pump}} \tag{31}$$

Where the absorbed ECRH power $P_{ECRH} = P_{cp}(2\ V_p)$ is given by

$$P_{ECRH} = \frac{P_{fusion}}{Q_{ECRH}} \text{ (MW)} \tag{32}$$

where Q_{ECRH} is given by eq. 30, where

$$P_{NB} = \frac{2\, n_p^2 \, \frac{4}{3}\pi r_p^3 \, E_{inj} \, (1.6 \times 10^{-16})}{(n\tau)_p} \quad (MW) \qquad (33)$$

(r_p in m)

with $(n\tau)_p \quad 6.3 \times 10^{10} \, E_{inj}^{3/2} \, \log_{10} R_p \, (eff)$

(E_{inj} in keV)

being the plug ion particle confinement for hydrogen in the ion-ion scattering limit (small drag) with an effective mirror ratio

$$R_p(eff) = \left[\frac{R_p / \sqrt{1 - \beta_p}}{1 + \left(\frac{\phi_e + \phi_c}{E_{inj}} \right)} \right] \qquad (35)$$

that approaches unity as E_{inj} approaches the cutoff energy, and where

$$P_{pump} = \frac{2 \left(\frac{n_b}{2} \right)^2 \frac{4}{3} \pi r_b^3 \, T_{ic} (1.6 \times 10^{-16})}{2.5 \times 10^{10} \, T_{ic}^{3/2}} \, (MW) \qquad (36)$$

is the ion pump power (absorbed) with r_b in meters and T_{ic} in keV.

The resulting plasma parameters for the three ion temperature cases are given in Table A. The important point to note is that both the Q and wall loading Γ are relatively insensitive to the ion temperature and beam injection energy. However, the thermal barrier filling time τ_g increases nearly an order of magnitude going from T_{ic} = 20 keV to T_{ic} = 60 keV.

Table A

TMR PLASMA PARAMETERS

	Case 1	Case 2	Case 3
T_{ic} (keV)	20	40	60
T_{ec} (keV)	20	40	52
I_s/I_c	20	1.6	0
$(n\tau)_c$ $cm^{-3}sec$	1.75×10^{15}	9.0×10^{14}	1.2×10^{15}
ϕ_c (keV)	90	125	173
ϕ_e (keV)	117	244	356
ϕ_b (keV)	45	83	108
β_p	0.50	0.64	0.70
E_{inj} (keV)	150	200	300
E_p (keV)	375	500	750
n_c (cm^{-3})	2.20×10^{14}	1.53×10^{14}	1.20×10^{14}
n_p (cm^{-3})	6.22×10^{13}	5.15×10^{13}	4.06×10^{13}
n_b (cm^{-3})	2.3×10^{13}	1.9×10^{13}	1.5×10^{13}
T_{ep} (keV)	136	217	293
r_c (m)	0.85	0.87	1.05
r_b (m)	1.22	1.33	1.70
r_p (m)	0.51	0.64	0.83
B_c (T)	2.33	2.98	3.11
B_b (T)	0.563	0.638	0.593
$(n\tau)_p$ $cm^{-3}sec$	8.7×10^{12}	1.23×10^{13}	3.96×10^{13}
both plugs: P_{ECRH} (MW)	47	50	57
both plugs: P_{NB} (MW)	12	15.2	10
both plugs: P_{PUMP} (MW)	1.7	1.8	1.9
Plasma Q (overall)	24.7	22.5	21.8
Barrier Filling Time τ_g (msec)	73	260	550
Neutron Wall Loading Γ (MW/m^2)	3.3*	3.6*	3.1*
r_{wall} (m)	1.2	1.1	1.3

* This value can always be reduced by increasing the first wall radius if such proves to be cost effective from the wall lifetime point of view.

Since τ_g is the time any pumpout mechanism must compete with, the implied pump power dissipated in the driver, as opposed to the P_{pump} which is absorbed in the plasma, can be expected to decrease as the temperatures are increased. Thus any technology associated with higher beam injection energies required for the higher ion temperatures is traded off against pump technology made easier by longer τ_g at the higher temperatures. As a compromise, case (2) at T_{ic} = 40 keV, E_{inj} = 200 keV, and τ_g = 260 msec, would appear to be the best choice. It must be emphasized that the neutral beam injection energies given in Table A are the bare minimums that would be possible at those temperatures without an A cell. With A cells added to the ends of the plugs to divide up the plug potential drop, somewhat lower beam energies could be used, but with the added complexity and cost of the A cells the payoff may not be worth it. With 50% higher injection energies than those given in Table A, the plug $(n\tau)_p$'s would increase an order of magnitude due to large percentage increases in $R_{eff} - 1$, resulting in 10 times less beam power required, and 10 times less beam current density. To do this, however, requires neutral beams based on negative ion sources. If it were absolutely necessary, positive-ion neutral beam systems with direct recovery might be usable in case 1, but with a severe penalty in beam efficiency (with hydrogen at 150 keV, neutralizer efficiencies are only 10%).

To take a preliminary look at some of the power system and economic parameters that go with the plasma parameters in Table A, we compute power flows with the following assumptions:

(1) Blanket neutron energy multiplication

$M = 1.2$

(2) Blanket thermal efficiency

$\eta_{TH} = 0.33$

(3) ECRH tube efficiency

$\eta_{ECRH} = 0.67$

(assuming depressed electron collector potentials and thermal recovery of collector heat at 33%)

(4) Neutral beam efficiency

$\eta_{NB} = 0.67$

(5) Direct Converter Efficiency

η_{DC} = 60% direct, single stage
+ 33% thermal recovery

The neutral beam trapping fraction is computed from

$$f_t = 1 - e^{-\gamma} \tag{37}$$

where $\gamma = 1.85 \times 10^{-12} n_p r_p E_{inj}^{-.91}$

with n_p in cm^{-3}, r_p in m, E_{inj} in keV.

For the assumed compressional pumping, the quantities of interest are the magnetic energy stored in the pulsed coil

$$W_{coil} = 2\pi r_b^3 \frac{(B_{mb} - B_b)}{2\mu_o} 10^{-6} \text{ (MJ, each coil).} \tag{38}$$

Assuming a transfer efficiency of 90% for this stored energy between the coil and rotating machinery such as homopolars, the average pulsed coil dissipated power is

Table B

TMR ENGINEERING PARAMETERS

		Case 1	Case 2	Case 3
	plasma Q	24.7	22.5	21.8
	$\Gamma MW/m^2$	3.3*	3.6*	3.1*
	τ_g (millisec)	73	260	550
	(each coil) W_{coil} MJ	54	66	143
both ends	P_{coil} (MW e)	148	50	52
both ends	P_{ECRH} (trapped) (MW)	47	50	57
both ends	P_{ECRH} (electrical) (MWe)	70.5	75	85.5
both ends	P_{NB} (trapped) (MW)	12	15.2	10
both ends	P_{NB} (incident) (MW)	26	39	34
both ends	P_{NB} (electrical) (MW e)	39	58.5	51
	$P_{Gross\ electric}$ (MW e)	744	749	750
	$P_{recirculating}$	258	183.5	188.5
	$f_{recirculating}$	0.347	0.245	0.251
	f_{trap}	0.46	0.39	0.29
	Direct Converter MW e)	216	220	221
	Electric Power (direct)			
	P_{net} MW e)	486	566	561.5

* This value can always be reduced by increasing the first wall radius if such proves to be cost effective from the wall lifetime point of view.

$$P_{coil} \simeq \frac{0.1\ (2\ W_{coil})}{\tau_g}\ \text{MW (e)} . \qquad (39)$$

The results for the engineering parameters of the three reactor cases are given in Table B. The minimum coil power P_{coil} is significantly reduced in case (2) compared to case (1) as expected from the longer τ_g in case (2). However P_{coil} is not further reduced in going to case (3) at still longer τ_g since the coil radius, volume, and stored energy W_{coil} is also increased enough to offset the longer τ_g. Thus for minimum neutral beam voltage at minimum coil power, case (2) appears to be the choice. Note that while the neutral beam trapped power is small in comparison to the absorbed ECRH power, the neutral beam electrical power consumption is more comparable to the ECRH electric power due to the finite neutral beam trapping efficiency. Note that in cases (2) and (3) the direct electric output from the direct converter is sufficient to supply all the recirculating electric power. Since the single-stage direct converter is simple and low cost, this will have a significant impact on the cost associated with the recirculating electric power. In particular, since the ECRH gryotron tubes' main power requirement (to the electron collector) can in principle be unregulated, and the electron beam voltage matched to the direct converter output, very little electric power conditioning equipment such as transformers, rectifiers, regulators, etc. may be needed for the ECRH, which is the primary electric power consumer in this type of reactor. Thus substantial cost savings may result.

To scale from these 500 MW(e) reactor outputs to larger reactor outputs, note that since the center cell is ignited,

$$Q \propto L_c \propto P_{fusion},$$

so that approximately we have

$$f_{recirculating} \propto 1/L_c \propto 1/P_{net}.$$

In conclusion it appears that TMR's with thermal barriers can have substantially increased Q and wall loading at smaller size, lower fields and lower beam injection energies than in previous designs. New technology requirements for ECRH heating and compressional ion pumping, while not precisely defined until detailed designs are made, would appear to be quite manageable. Neutral beam systems based on negative ions, while not absolutely essential, are still desirable.

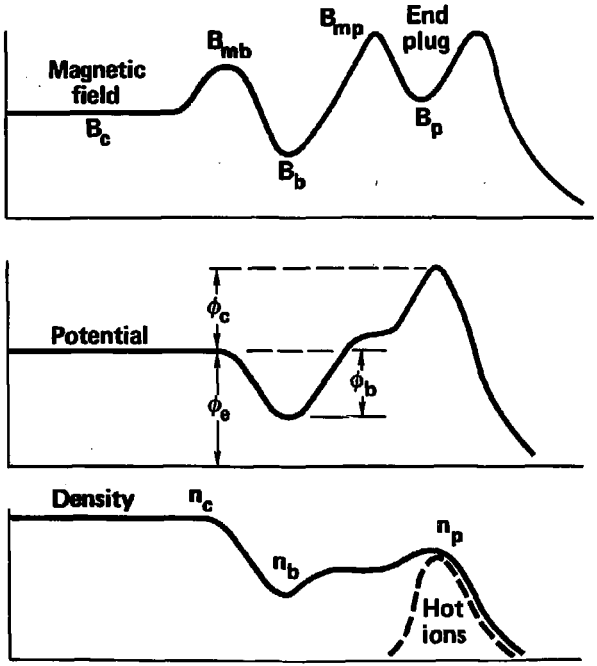
Magnetic field
B_c
B_{mb}
B_b
B_{mp}
End plug
B_p
Potential
ϕ_c
ϕ_e
ϕ_b
Density
n_c
n_b
n_p
Hot ions

Figure 1

IMPROVED TANDEM MIRROR

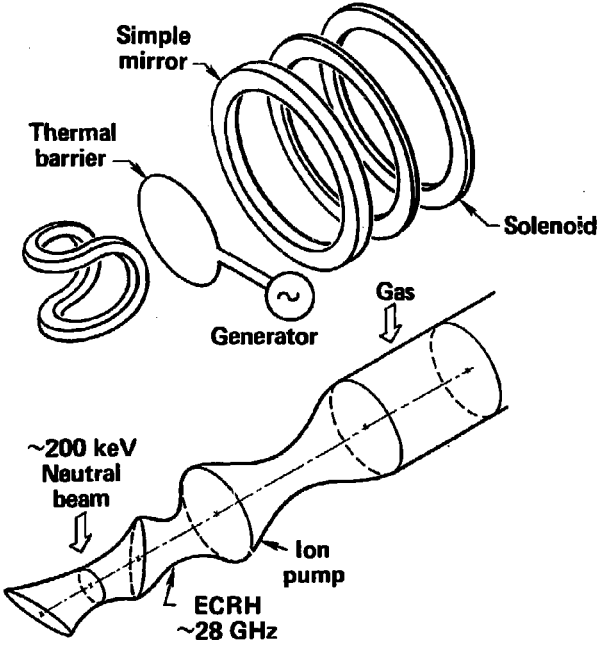

Figure 2

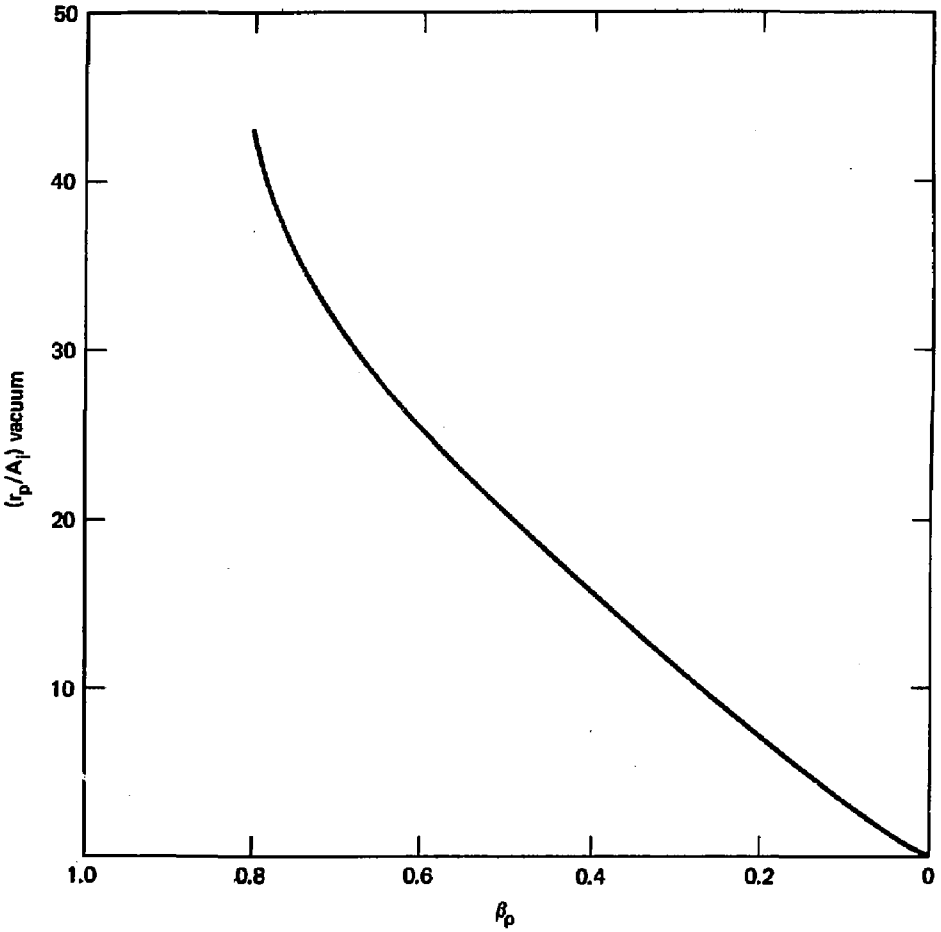

Figure B1. DCLC Stability Boundary for $\bar{E}_p + T_{ep} = 1$ Mev (Hydrogen)

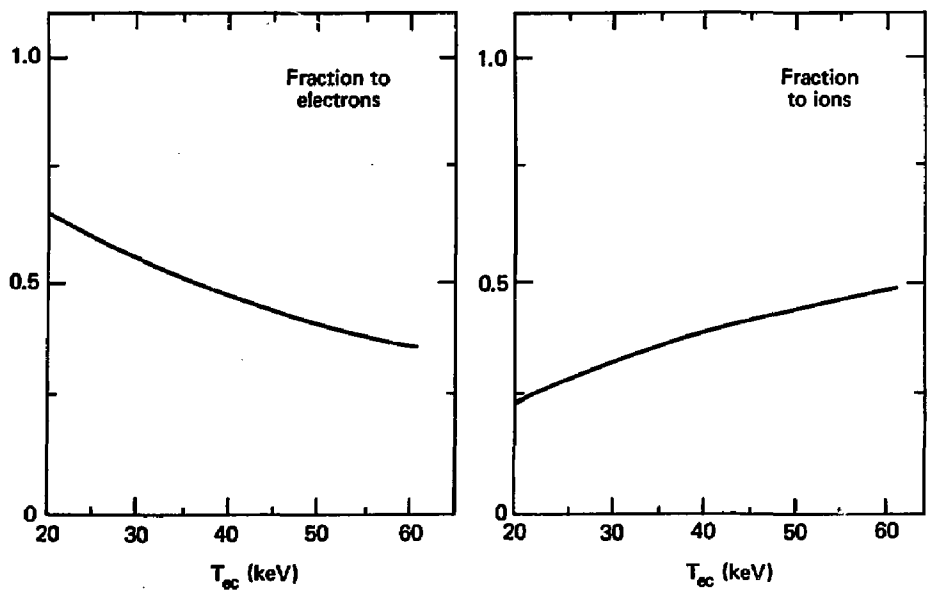

Figure B2. Alpha Particle Energy Deposition

U.S.GPO:1979-689-060/2005